

Statistical Evaluation of Modified Electrical Resistance Change Method for Delamination Monitoring of CFRP Plate

Atsushi Iwasaki^{1,*} and Akira Todoroki²

¹*Department of Mechanical Engineering, University of Tokyo, 7-3-1 Hongo Bunkyo-ku, Tokyo 113-8656 Japan*

²*Department of Mechanical Sciences and Engineering, Tokyo Institute of Technology, 2-12-1, Ohokayama, Meguro, Tokyo 152-8552, Japan*

The present paper employs the electric resistance change method for monitoring the location and size of a delamination crack in graphite/epoxy composite laminates. The authors have revealed that the electric resistance change method with response surfaces is very effective experimentally and analytically. For the estimations of delamination locations, however, large error of the estimations still remains. FEM analyses revealed that the standardizations of the electric resistance changes are very effective to obtain high performance identifications. In this study, the new electric resistance change method of high performance identification of delaminations is applied to a plate-type specimen with an embedded delamination of cross-ply and quasi-isotropic laminates. Ten electrodes made from copper foil are mounted on the specimen top surfaces. The electric resistance changes are measured using a conventional strain gage amplifier. Response surfaces are adopted as a tool for solving inverse problems to estimate the location and size of delamination crack from the measured electric resistance changes of all segments between electrodes. Statistical analysis was performed to result of identification using the response surface. As a result, the present method successfully provides estimations of location and size of the embedded delamination for graphite/epoxy laminated composites.

Keywords delamination monitoring · electric resistance · composite material · response surface · smart structure

1 Introduction

Carbon-fiber reinforced plastics (CFRP) have high specific tensile strength and stiffness, and are good for the major structure of airplanes and space instruments. The intensity between layers of CFRP is weak and a delamination crack between layers is produced by a comparatively slight

impact. The delamination cracks are invisible and cause decrease of compression strength of laminated composites. Therefore, a diagnostic method for the delamination crack of laminated composite is required. A structural health monitoring system to diagnose the delaminations is one of the desired approaches for practical laminated composite structures.

*Author to whom correspondence should be addressed.
E-mail: iwasaki@fml.t.u-tokyo.ac.jp

Recently, an electric resistance change method was employed to identify the internal damage of CFRP laminates by many researchers [1–18]. The electric resistance change method does not require expensive instruments. Since the method adopts reinforcement carbon fiber itself as sensors for damage detections, this method does not cause reduction of static strength or fatigue strength, and it is applicable to existing structures.

The authors have already experimentally investigated the applicability of the electric resistance change method for measurements of delamination crack length of the edge cracks of delamination resistance tests [19,20]. For practical composite structures, however, delamination cracks are usually embedded cracks. The embedded cracks of the beam-type specimens were also experimentally detected by the electric resistance change method by Todoroki using graphite/PEEK composites [21]. In order to investigate the effect of orthotropic electric resistance on the delamination monitoring of cross-ply laminates, several FEM analyses have also been performed [22,23]. Beam-type specimens were employed to monitor delamination creations experimentally [24], and plate-type specimens of cross-ply laminates were also adopted to monitor the delamination creations experimentally [25]. For the plate-type specimens, estimated locations of delamination cracks were discrete levels instead of continuous coordinates to simplify the inverse problems. For these researches, a response surface method is adopted as a tool to solve the inverse problems: delamination location and size must be obtained from the measured electric resistance changes of multiple segments between electrodes. In this method, the performance of the estimations of delamination location was not sufficient compared to the estimations of delamination size.

In the previous study [26–29], therefore, a large number of FEM analyses of various delamination sizes and locations of beam-type specimens are performed to investigate the reason, and an improvement method is proposed for the data standardization method before making the response surfaces. The new method is applied to estimate the delamination location and size of

the beam-type specimens obtained from FEM analyses, and the performance has been shown to be excellently high.

In the present study, the new method is applied to the experimental data conducted previously to investigate the effect of the experimental error and a matrix crack created with a delamination [24]. In the experiments, two types of laminates of different stacking sequences are adopted: cross-ply laminates and quasi-isotropic laminates. An embedded delamination crack is created in a plate-type specimen on which multiple electrodes are mounted. Electric resistance changes of all of the segments between the electrodes are measured with a conventional strain gage amplifier. Using response surfaces, the actual location and size of a delamination crack is estimated as continuous values. Statistical analysis was performed to result in identification using the response surface. Applicability of the method for the estimation of continuous values of location and size of a delamination crack is statistically investigated in detail.

2 A New Electric Resistance Change Method

Practical graphite fiber in a unidirectional ply is serpentine as shown in Figure 1(a), and the ply is also serpentine as shown in Figure 1(b). The curved graphite fiber contacts with each other, and that makes a graphite-fiber network in a laminate. The contact network brings nonzero electric conductivity even in the transverse and thickness directions. The electric conductivity in the transverse direction is much lower than that of the fiber orientation. Abry et al. [11] and the authors [26] have revealed experimentally that the electric conductivity ratio of the transverse direction (σ_{90}) to the fiber direction (σ_0) is very small, and the electric conductivity ratio of the thickness direction (σ_t) to the fiber direction is smaller than that of the transverse direction. The example of the case of fiber volume fraction is 62% as shown in Table 1 [26].

When a delamination crack grows in the interlamina, the crack breaks the fiber contact network between plies. The breakage of the

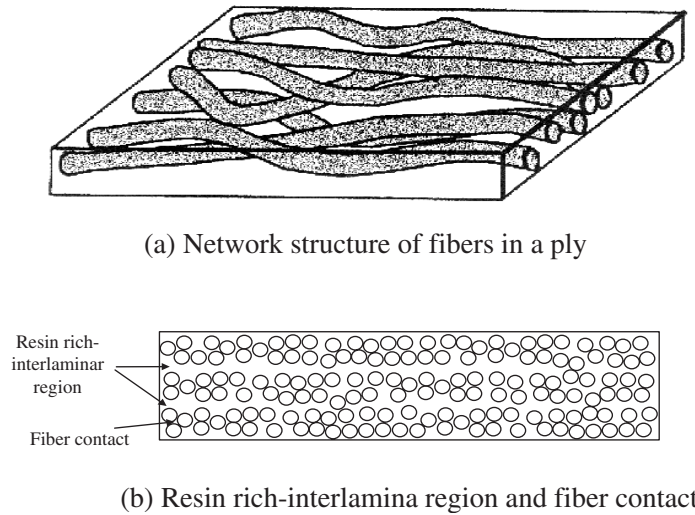


Figure 1 Schema of practical structure of graphite/epoxy composite.

Table 1 Measured orthotropic electric conductance of graphite/epoxy composite.

| | σ_0 (S/m) | σ_{90}/σ_0 | σ_t/σ_0 |
|----------------------|------------------|------------------------|----------------------|
| Electric conductance | 5500 | 3.7×10^{-2} | 3.8×10^{-3} |

contact network causes increase of the electric resistance of the CFRP laminates. Therefore, delamination crack can be detected by the electric resistance change of CFRP laminates.

Figure 2 reveals the schematic representation of the delamination monitoring system proposed by authors. Multiple electrodes are mounted on the specimen surface as shown in Figure 3. All of these electrodes are placed on a single side of the specimen. Usually it is impossible to place electrodes and lead wires outside of the aircraft structures. The location of the electrodes on the single side surface is representative of the location of electrodes in the thin aircraft shell-type aircraft structures. The authors performed several FEM analyses and revealed that the electric current should be charged in the fiber direction of the surface ply to monitor a delamination crack [26]. Electric resistance change of each segment between electrodes is measured with a conventional electric resistance bridge circuit as shown in Figure 4. The electric resistance changes between all of the segments are measured for

various cases of location and size of delaminations. Using the measured data, relations between electric resistance change and delaminations (location and size of delaminations) are obtained using response surfaces. Since the authors have revealed that the response surfaces give better performance than artificial neural networks for this inverse problem, the response surface method is employed here [27]. After the calculations of the response surfaces, location and size of a delamination can be estimated with the response surfaces from the measured electric resistance changes.

Let us consider the case of Figure 3. In this case, eight electric resistance changes ε_i ($i=1-8$) are measured at the segments. To create the response surfaces, a lot of experiments or calculations must be performed. From the experiments, a lot of data sets of delamination location (segment location, column location), size, and electric resistance changes are obtained. When quadratic polynomials are adopted, the response surfaces to estimate the delamination location (segment X , column Y) and size (a) are as follows:

$$X = \beta_0 + \sum_{i=1}^8 \beta_i \varepsilon_i + \sum_{i=1}^8 \sum_{j=i}^8 \beta_{ij} \varepsilon_i \varepsilon_j \quad (1)$$

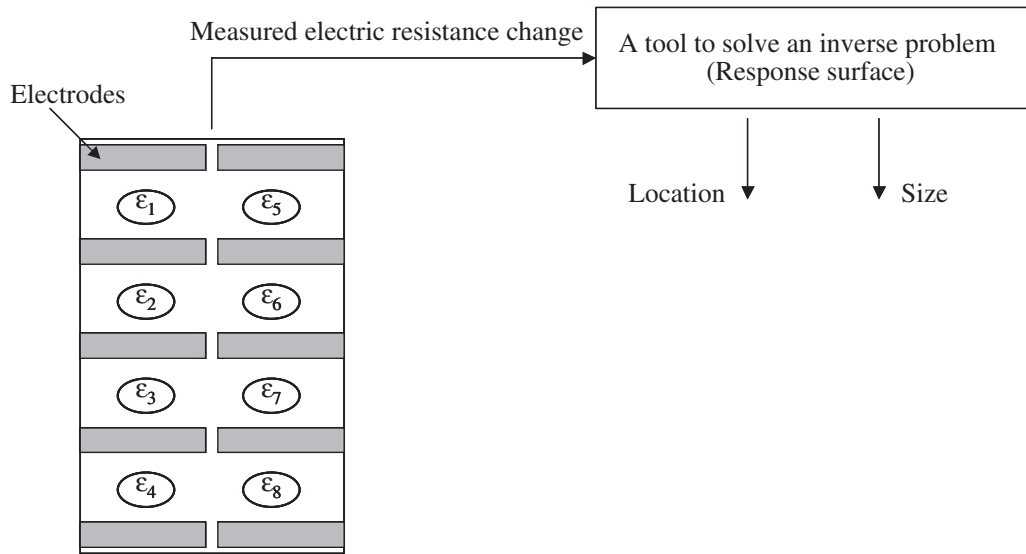


Figure 2 Schematic representation of delamination identification method using electric resistance change method with response surfaces.

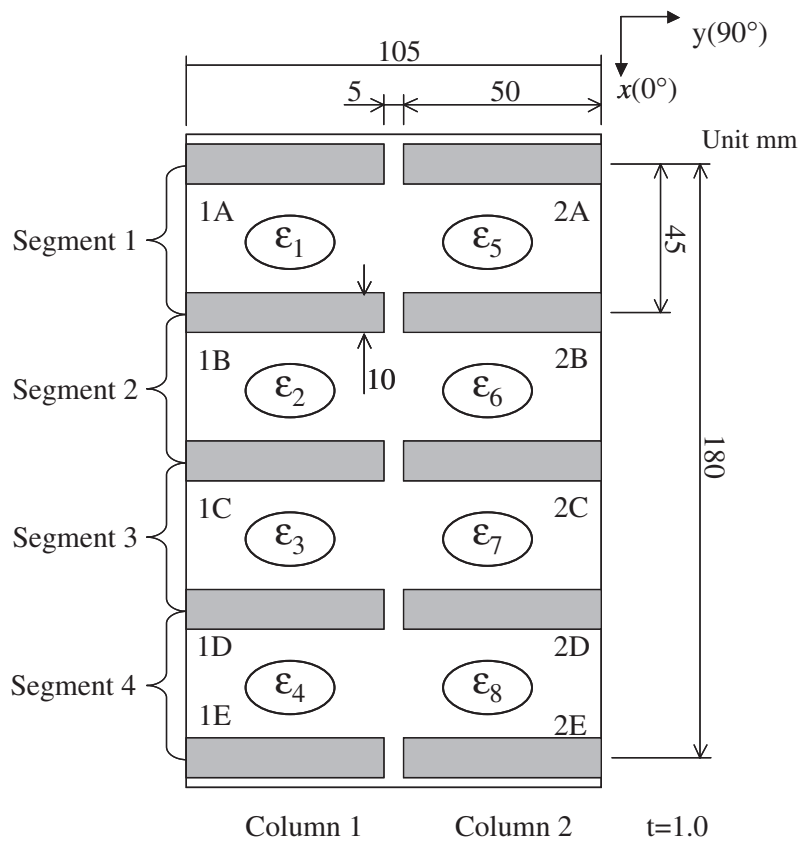


Figure 3 Specimen configuration.

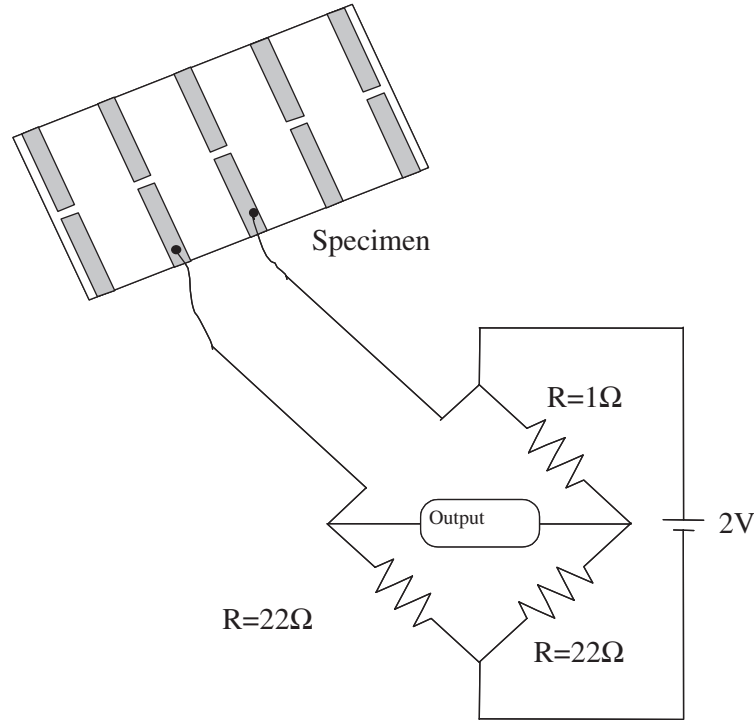


Figure 4 Electric bridge circuit.

$$Y = \beta_0 + \sum_{i=1}^8 \beta_i \varepsilon_i + \sum_{i=1}^8 \sum_{j=i}^8 \beta_{ij} \varepsilon_i \varepsilon_j \quad (2)$$

$$a = \beta_0 + \sum_{i=1}^8 \beta_i \varepsilon_i + \sum_{i=1}^8 \sum_{j=i}^8 \beta_{ij} \varepsilon_i \varepsilon_j \quad (3)$$

where, β_i ($i=0-8$) and β_{ij} ($i=1-8; j=1-8$) are regression coefficients and all the regression coefficients are obtained with the least square error method [30]. These estimations are called the previous method here. The lack of fit is evaluated with the adjusted coefficient of multiple determination R_{adj}^2 [30]. The R_{adj}^2 is usually lower than 1.0. Higher value of R_{adj}^2 means good fit. When the response surface shows very good fit, the R_{adj}^2 approaches to 1.0.

The authors have reported that the response surfaces may provide poor performance for estimations of delamination location for small delaminations [28]. The poor estimations are caused due to the fact that the obtained configurations of the electric resistance change distributions contain the information of both the delamination location and the delamination size.

The authors have proposed a new electric resistance change method with standardizations of electric resistance changes. The standardizations make independent configurations of the electric resistance changes of the delamination size. The new method enables us to obtain significantly higher performance estimations of the delamination location. In the case of Figure 2, the measured electric resistance changes can be regarded as a vector of eight elements: ε_i ($i=1-8$). The length of the vector η is defined as follows:

$$\eta = \sqrt{\sum_{i=1}^8 \varepsilon_i^2} \quad (4)$$

All of the elements are divided by η to obtain the standardized electric resistance changes vector (\mathbf{v}) as follows:

$$\mathbf{v} = \begin{pmatrix} v_1 \\ v_2 \\ \vdots \\ v_8 \end{pmatrix} = \begin{pmatrix} \varepsilon_1/\eta \\ \varepsilon_2/\eta \\ \vdots \\ \varepsilon_8/\eta \end{pmatrix} \quad (5)$$

With the standardized electric resistances, the response surface to estimate the delamination location is obtained as follows:

$$X = \beta_0 + \sum_{i=1}^8 \beta_i v_i + \sum_{i=1}^8 \sum_{j=i}^8 \beta_{ij} v_i v_j \quad (6)$$

$$Y = \beta_0 + \sum_{i=1}^8 \beta_i v_i + \sum_{i=1}^8 \sum_{j=i}^8 \beta_{ij} v_i v_j \quad (7)$$

For the estimations of the delamination size, the length of the vector is also of significant effect. Thus, the total number of variables of the response surface is increased by one as follows:

$$\begin{aligned} a = & \beta_0 + \sum_{i=1}^8 \beta_i v_i + \beta_9 \eta \\ & + \beta_{00} \eta^2 + \sum_{i=1}^8 \beta_{0i} \eta v_i + \sum_{i=1}^8 \sum_{j=i}^8 \beta_{ij} v_i v_j \end{aligned} \quad (8)$$

These new response surfaces for estimations are called the new method here. In the present paper, the terms of the response surfaces that reduce the value of R_{adj}^2 are deleted using t -statistics [30].

3 Specimens and Experimental Procedures

3.1 Specimens

The material used in the present paper is unidirectional graphite/epoxy prepreg. The type of the unidirectional prepreg sheet is TR340M150ST produced by Mitsubishi-Rayon Co. Ltd. Using the prepreg, cross-ply laminates of $[0_2/90_2]_s$ and quasi-isotropic laminates of $[0/45/-45/90]_s$ were fabricated. The fiber volume fraction is approximately 0.5. Thickness of the laminates is approximately $t=1$ mm. Cure condition is $130^\circ\text{C} \times 1.1 \text{ MPa} \times 1 \text{ h}$ using a hot press. In order to measure electric resistance changes using a two-probe method, reliable electrodes are indispensable. In order to produce the reliable electrodes, a rectangular copper foil of 0.02 mm thickness is mounted on the prepreg laminates,

and these electrodes are co-cured with the laminate. From the laminates, rectangular plate-type specimens of length 200 mm and width 105 mm were produced, as shown in Figure 3. The multiple electrodes are mounted on a single surface of the specimen in the present study as previously mentioned.

3.2 Electric Circuit

Since electric resistance change due to a delamination crack creation is very small, the electric resistance change is measured with the electric resistance bridge circuit as shown in Figure 4. As easily recognized, the bridge circuit is quite similar to that of the conventional strain gages. Therefore, conventional strain gage amplifiers are adopted for measurements of electric resistance change of the specimens without any changes. That brings that the output of the instrument is 'strain,' but it does not mean deformation of the specimens. The output 'strain' means electric resistance change ratio here. The electric resistance change ratio is expressed using output 'strain' data ε as follows:

$$\frac{\Delta R}{R} = k\varepsilon \quad (9)$$

where, ΔR is the electric resistance change due to a creation of a delamination crack, R is an initial electric resistance, k is a gage factor, and ε is a measured output 'strain.' Usually, the gage factor adopted for the conventional strain gage amplifier is 2. In order to obtain higher output 'strain' data, the electric resistance change ratio $\Delta R/R$ should be large. Since the electric resistance change (ΔR) is very small and the measured initial electric resistance (R) of the specimen is approximately 1Ω the electric resistances of the bridge circuit are arranged from the normal circuit for conventional strain gages. By trial and error, electric resistance of 22Ω is selected as another resistance R in this bridge circuit. Since the measured output is ε , ε is called the electric resistance change ($v = \Delta R/R/k$) in the present study though it still includes the effect of the gage factor.

3.3 Experimental Procedures

In order to create a delamination crack in each plate-type specimen, an indentation test is employed here. As shown in Figure 5, an indentation-type jig and cylindrical support is adopted here. By changing the diameter of the cylindrical support jig from 10 to 50 mm, several sizes of delamination were created in the plate-type specimen. Since the method employs a two-probe method, the electrodes are avoided for the indentation tests to prevent electric resistance change at the electrodes. This could be improved when a four-probe method is employed. The indentation point is loaded from the opposite side surface where the electrodes are mounted. This is to simulate the placements of electrodes inside of the structures and the impact load that creates a delamination comes from the outside. Since the specimen is a thin laminate, the loading creates a large delamination crack in the 0–90° interface near the electrodes.

After creating a delamination crack, electric resistance changes of all segments between electrodes were measured using a conventional strain amplifier. Delamination location and size were measured using an ultrasonic C-scan image. The delamination location is decided at the center point of the delamination crack from the specimen end. Since the location in the plate-type specimen has two directions, two directions of x -direction (0°-direction) and y -direction (90°-direction) are decided for the identification of the delamination location. The delamination size corresponds to the maximum diameter of the delamination crack.

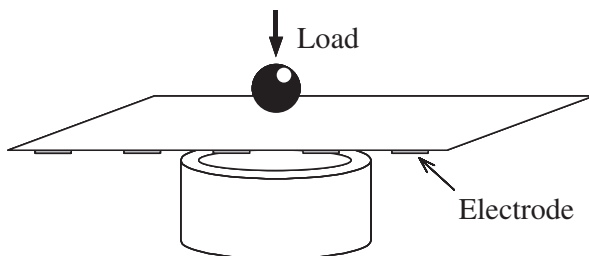


Figure 5 Indentation procedure of the laminates to create a delamination crack.

4 Results and Discussion

4.1 Delamination and Electric Resistance Changes

Typical examples of the C-scan images of the created delamination cracks of cross-ply laminates and quasi-isotropic laminates are shown in Figure 6. These delamination cracks include the matrix cracks, and these are completely embedded in the laminates like practical delamination cracks. From the visual inspection, no fiber breakage is observed. As shown in Figure 7, a larger delamination crack is created near the surface where the electrodes are mounted. This is because the indentation loading is performed from the opposite surface where the electrodes are mounted, as explained by Suemasu and Majima [31]. Since the laminates are thin, location of the delamination along the thickness direction is almost the same for all specimens. In the present study, therefore, only the location

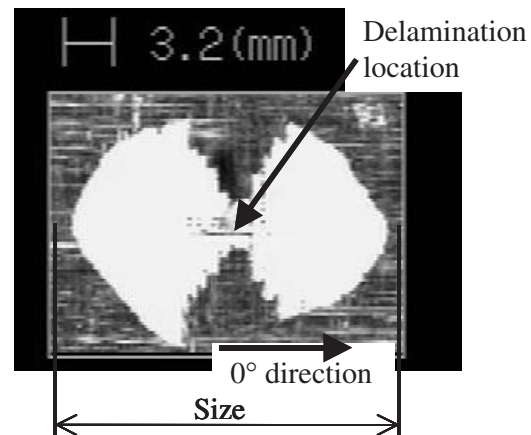


Figure 6 C-scan image of delamination crack.

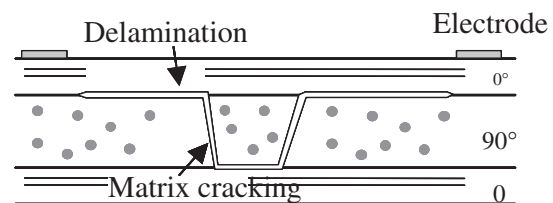
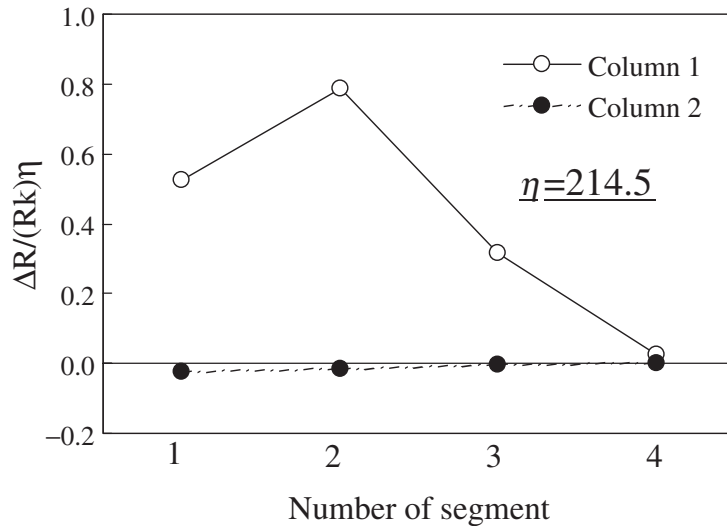


Figure 7 Schematic image of cross section of delamination.

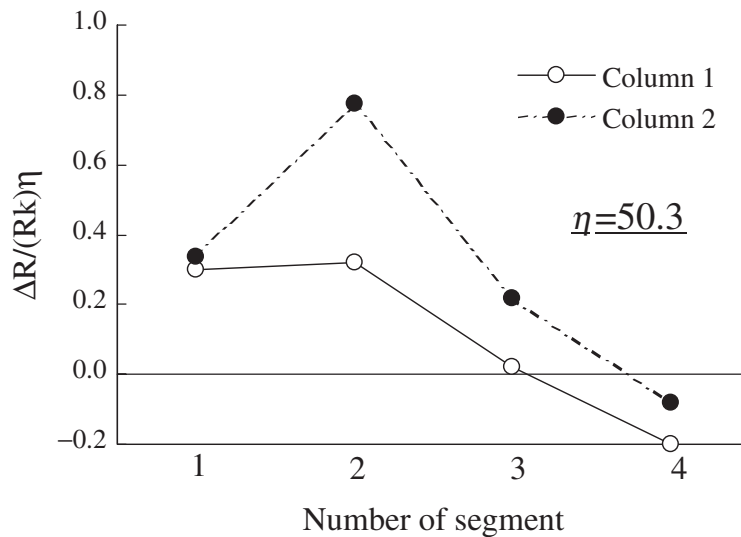
of the x - and y -directions of the delamination is discussed.

Typical experimental results obtained after delamination creations are shown in Figures 8 and 9. The measured electric resistance changes of all the segments between electrodes of the cross-ply laminate is shown in Figure 8(a) and (b). The measured electric resistance changes of all

the segments between electrodes of the quasi-isotropic laminate is shown in Figure 9(a) and (b). Figure 8(a) and 9(a) show the results in the case of a delamination of approximately 20 mm in the second segment ($x=68.4$ mm or 67.1 mm) and in the first column ($y=22.2$ mm or 22.4 mm). Figures 8(b) and 9(b) show the results in the case of a delamination of approximately 20 mm



(a) Delamination exists at column 1, segment 2
($X=68.4$, $Y=22.2$ $a=26.0$)



(b) Delamination exists at the middle of both columns, segment 2
($X=66.7$, $Y=54.5$ $a=23.6$)

Figure 8 Typical measured standardized electric resistance change ratio of cross-ply laminate.

between the first and second columns ($y=54.5$ or 50.6 mm) and in the second segment ($x=66.7$ or 67.5 mm). For all these figures, the ordinate is the measured electric resistance ratio of each segment and the abscissa is the segment number. The solid lines show the results of the first column and the broken lines show the results of the second column.

For both laminates, only the electric resistances of the first column change and the electric resistances in the second column do not change when the delamination is located in the first column (the solid line cases). In this experiment, before and after creation of the damage, the error of average $-0.81[dR/R \cdot k]$ and distribution 4.71 were measured at the cross-ply specimens. And the error of average 0.04 and distribution 6.12 were measured at the angle-ply specimens. Fluctuations of the value of column 2 of Figures 8(a) and 9(a) are within these ranges. The ranges of the errors are calculated from unstandardized value.

On the other hand, when the delamination is located between the first and second columns (see Figures 8(b) and 9(b)), electric resistance changes in the two columns are measured. Although the delamination exists in the second segment in all cases, electric resistance changes in the first and third segments are measured. Moreover, in Figure 9(b), the electric resistance change of the first segment is larger than the second segment.

The electric resistance changes in the adjacent segments where delamination does not exist are due to the strong orthotropic electric conductance of graphite/epoxy laminates. This strong orthotropic electric conductance brings electric resistance changes in the adjacent segments.

It causes the identification of delamination difficult that a maximum in the electric resistance change does not always imply the existence of a delamination in the segment. Similar electric resistance changes are observed in the FEM analyses of beam-type specimens [26]. From this complexity, it is easily recognized that the estimation of the location of a delamination by a continuous value is a quite difficult problem.

The electric resistance change values of the cross-ply laminates are larger than those of the quasi-isotropic laminates by a factor of three.

This is owing to the delamination location in the thickness direction. For the quasi-isotropic laminates, the delamination exists at the interface between the 45° ply and -45° ply that locates far from the surface.

4.2 Identification of the Delamination Location

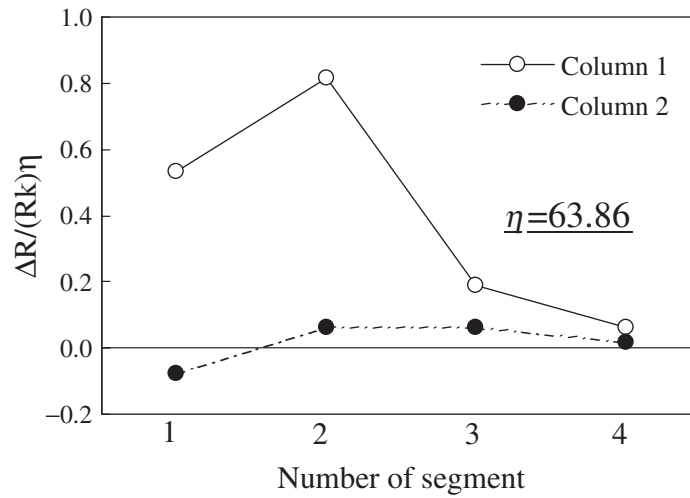
Using the measured electric resistance data sets (number of the data sets is 64), response surfaces to estimate location of the delamination crack from measured electric resistance changes are obtained. In order to estimate the location of delamination crack in a plate, we need two response surfaces; x -direction and y -direction. For the cross-ply laminates, the adjusted coefficient of multiple determinations R_{adj}^2 of x -direction is 0.953 and the R_{adj}^2 of y -direction is 0.925 . For the quasi-isotropic laminates, the R_{adj}^2 of the response surface of x -direction is 0.956 and the R_{adj}^2 of y -direction is 0.967 . The approximations for the location of delamination are quite good.

For each laminates, estimations of the delamination location using response surfaces shown in formulas (6) and (7) are performed. The probability distribution of the residual error of estimations are shown in Figures 10 and 11, respectively. For the figures, the ordinate is the residual error of estimation and the abscissa is the probability. The solid line is normal distribution $Z_{0,\sigma}$, where σ is standard deviation of residual error. The standard deviations of residual error of each laminates are shown in Table 1. As shown in Figure 10 and 11, residual error of estimation presents a good agreement with normal distribution.

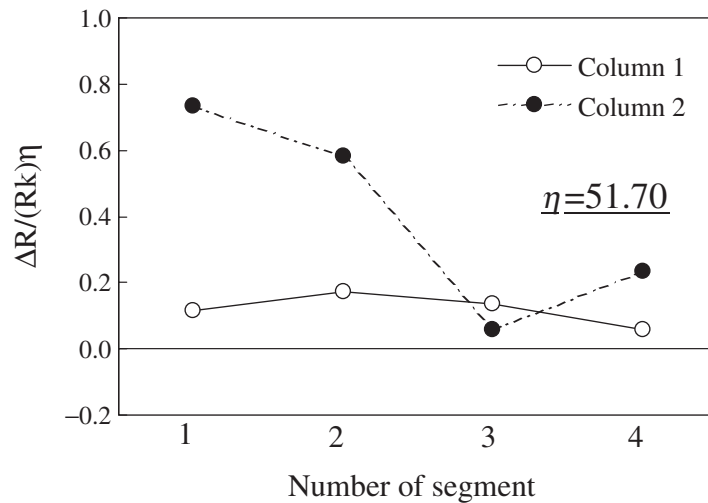
Test of fitness of distribution is performed as a χ^2 test, since y_0 derived from the following formula follows χ^2 distribution:

$$y_0 = \sum_i^k \frac{(f_i - F_i)^2}{F_i} \quad (10)$$

where, k is the number of categories of discrete distribution, f_i is the sample size contained in each category, and F_i is the expected size derived from a theoretical distribution. Since F_i must



(a) Delamination exists at column 1, segment 2
(X=67.1.4, Y=20.1 a=22.4)



(b) Delamination exists at the middle of the both columns, segment 2
(X=67.5, Y=50.6 a=21.0)

Figure 9 Typical measured standardized electric resistance change ratio of quasi-isotropic laminate.

exceed 5.0, experimental distribution is divided into 12 categories. The y_0 -values derived from experimental distribution are (5.84, 8.70, 15.2, 8.22) for (cross-ply x -direction, cross-ply y -direction, angle-ply x -direction, angle-ply y -direction). In the test, 5% critical value is $\chi^2_{11}^{0.05} = 19.7$. Since y_0 does not exceed the critical value, each distribution of estimated error follows normal distribution.

Since the residual error of the estimation follows normal distribution, error band of estimation is calculated from 99% confidence interval of normal distribution $Z_{0,\sigma}^{0.995}$. In the present result, the error bands of cross-ply laminate are 15.6 mm in the x -direction and 11.8 mm in the y -direction and of quasi-isotropic laminate are 15.4 mm in the x -direction and 7.8 mm in the y -direction.

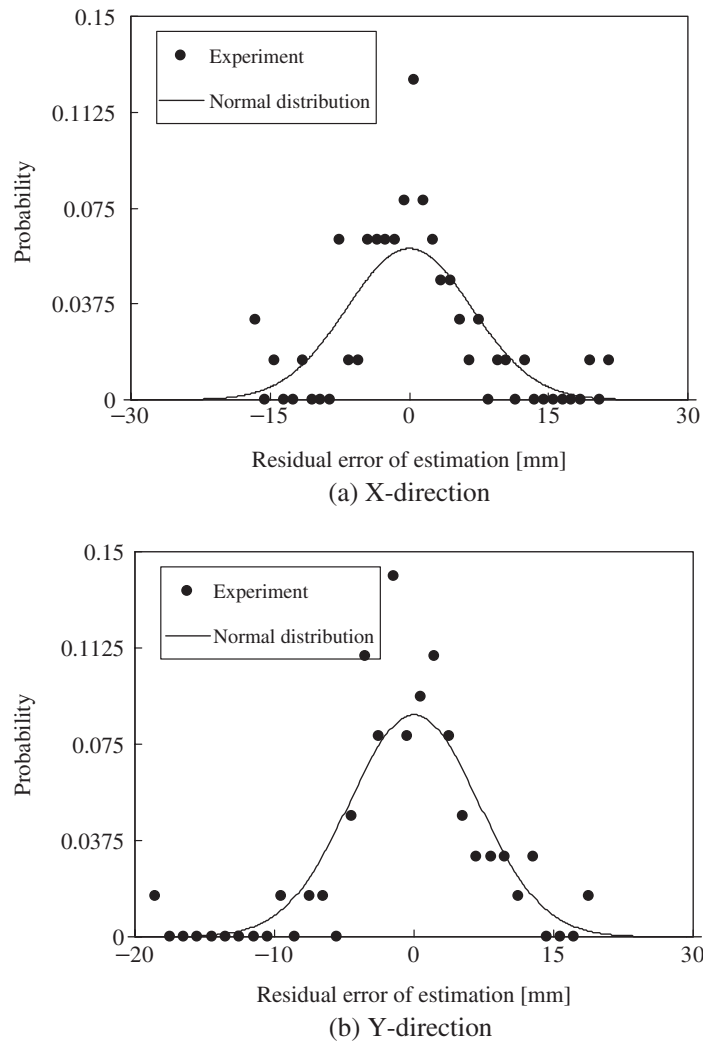


Figure 10 Residual error of estimation of delamination location for cross-ply laminate.

Figures 12 and 13 show error band of estimation of present method and previous study by formulas (1) and (2) [25]. For the figures, the solid line is probability distribution estimated from standard deviation of present method and the dotted line is the distribution of a previous method. The error band is decided from standard deviation of the error of estimation (shown in Table 2) and 99% confidence interval. The error band of estimation of the present method is smaller than the previous method. The error band of estimation of this

method and the previous method are shown in Table 2. As shown in the table, the error band of the present method is three times smaller than that of the previous one. In the present method, the error band of x - and y -directions are also 15 and 7 mm, which is slightly smaller than the spacing of the electrode segment ($50 \times 45 \text{ mm}^2$). From these results, we can conclude that the estimations of delamination location with modified electric resistance method improve the diagnostic accuracy of the delamination location.

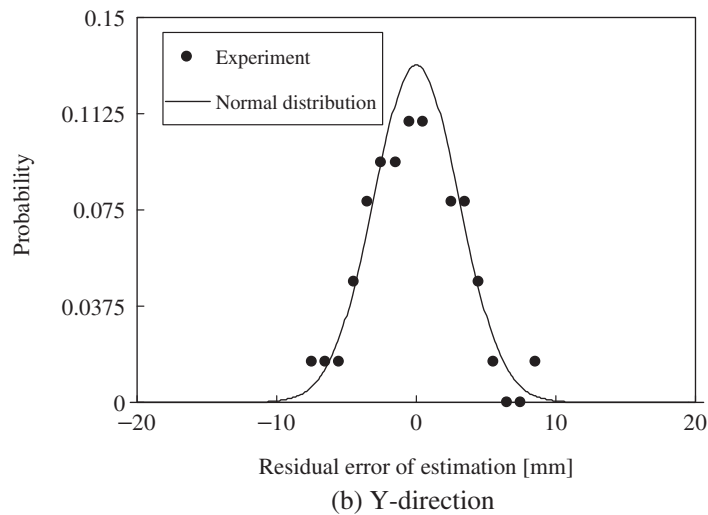
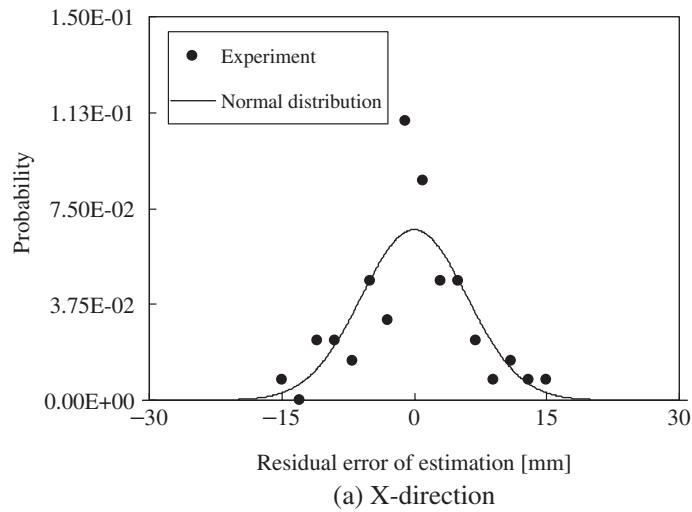


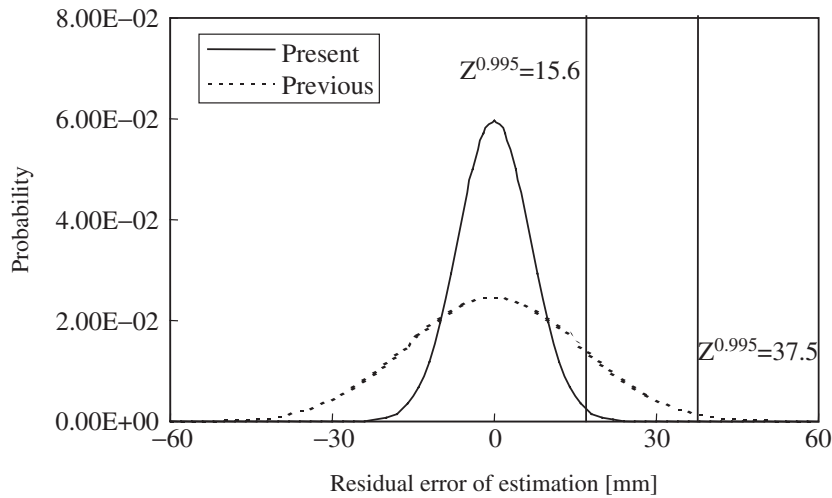
Figure 11 Residual error of estimation of delamination location for quasi-isotropic laminate.

4.3 Identification of the Delamination Size

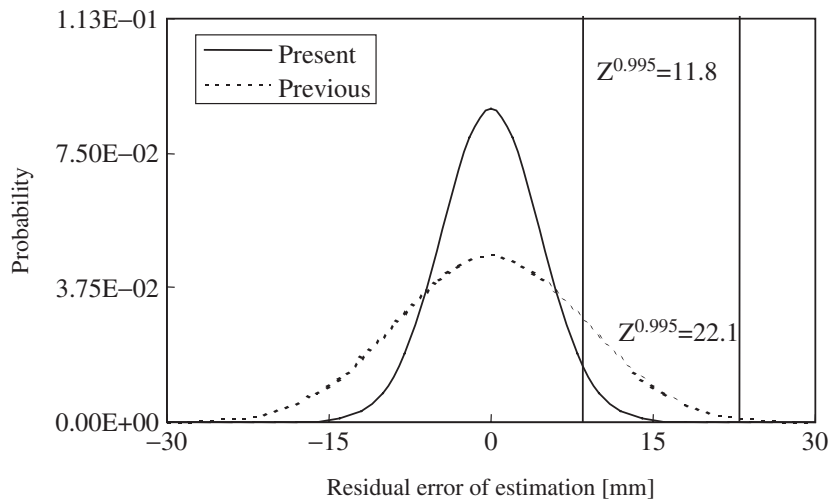
For the identification of the size of the delamination crack, we use response surface shown in formula (8). For the cross-ply laminates, the adjusted coefficient of multiple determinations R_{adj}^2 is 0.816, and the R_{adj}^2 for the quasi-isotropic laminates is 0.818. Both response surfaces give good approximations.

Results of estimation of both type of laminates are shown in Figures 14 and 15, respectively. The ordinate is the residual error of

estimation and the abscissa is the probability. The standard deviations of residual error of each laminates are shown in Table 3. As shown in Figures 14 and 15, residual error of estimation presents a good agreement with normal distribution $Z_{[0,\sigma]}$. Standard deviations of the present and previous methods which use response surface of formula (3) are shown in Table 3. Figures 16 and 17 show probability distribution of residual error of estimation of both methods estimated from standard deviation. In these cases, the y_0 values derived from experimental distribution are (5.62, 9.40) for (cross ply, angle ply).



(a) X-direction



(b) Y-direction

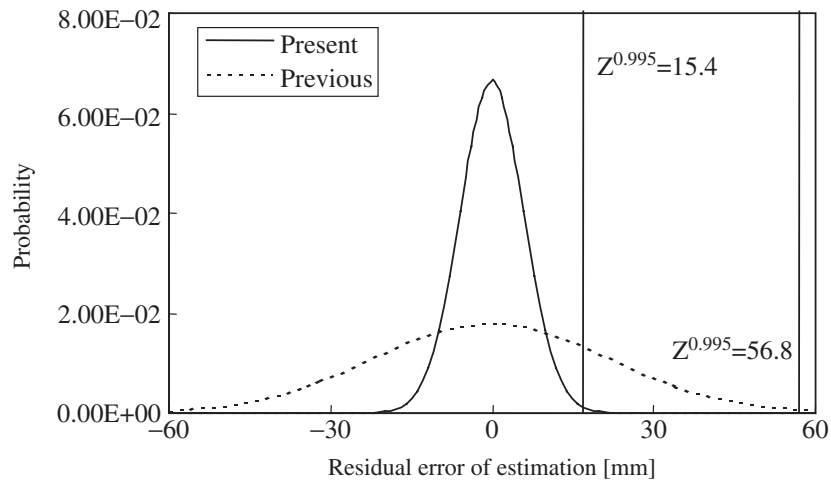
Figure 12 Error band of estimation of delamination location for cross-ply laminate.

Since y_0 does not exceed the critical value, each distribution of estimated error follows normal distribution. The error band which was decided from the 99% confidence interval of the probability distribution is shown in Table 3. As shown in the table, the error band of both methods is almost the same and improvement in accuracy was not observed.

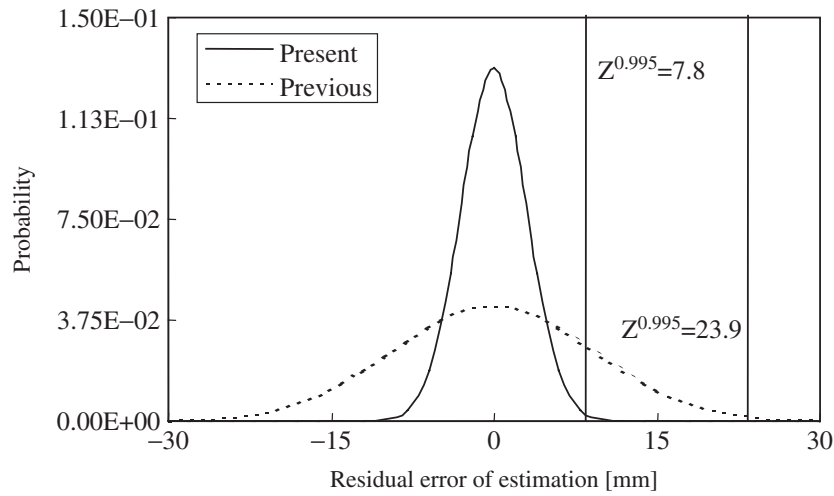
Since the measurement of the delamination size with the ultrasonic C-scan image has an error of approximately 3 mm, practical estimation

performance is defined that estimation error of 3 mm is tolerance for practical use.

As shown in these figures, most of the data locate inside of the error bands of 3 mm. For the cross-ply laminates, the practical performance of estimations is 96.9%, and for the quasi-isotropic laminates, the practical performance of estimations is 95.3%. From these results, we can conclude that the estimations of delamination size with modified electric resistance method are excellent.



(a) X-direction



(b) Y-direction

Figure 13 Error band of estimation of delamination location for quasi-isotropic laminate.

Table 2 Measured statistics and accuracy of estimation of delamination location.

| | <i>Data</i> | – | <i>Average E</i> | <i>Standard deviation σ</i> | <i>Error band</i> | <i>Improvement of accuracy</i> |
|-----------------|--------------|----------|------------------|-----------------------------|-------------------|--------------------------------|
| Cross-ply | Raw data | <i>X</i> | 0 | 259.7 | ±37.4 | – |
| | | <i>Y</i> | 0 | 73.7 | ±22.1 | – |
| | Standardized | <i>X</i> | 0 | 44.8 | ±15.6 | 2.41 |
| | | <i>Y</i> | 0 | 20.9 | ±11.8 | 1.88 |
| Quasi-isotropic | Raw data | <i>X</i> | 0 | 487.0 | ±56.8 | – |
| | | <i>Y</i> | 0 | 85.9 | ±23.9 | – |
| | Standardized | <i>X</i> | 0 | 35.8 | ±15.4 | 3.69 |
| | | <i>Y</i> | 0 | 9.2 | ±7.8 | 3.05 |

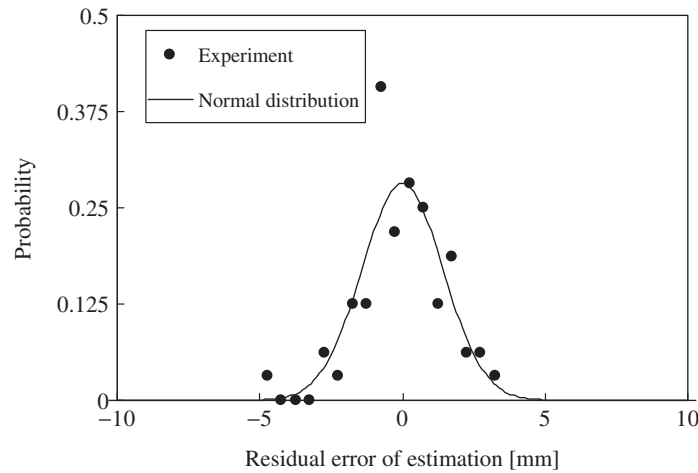


Figure 14 Residual error of estimation of delamination size for cross-ply laminate.

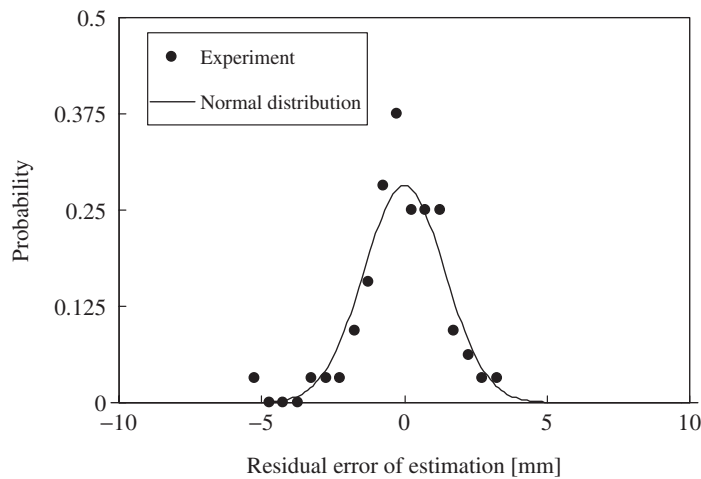


Figure 15 Residual error of estimation of delamination size for quasi-isotropic laminate.

Table 3 Measured statistics and accuracy of estimation of delamination size.

| | <i>Data</i> | <i>Average E</i> | <i>Standard deviation σ</i> | <i>Error band</i> | <i>Improvement of accuracy</i> |
|-----------------|--------------|------------------|---|-------------------|--------------------------------|
| Cross-ply | Raw data | 0 | 2.2 | ± 3.8 | |
| | Standardized | 0 | 2.5 | ± 3.7 | 1.05 |
| Quasi-isotropic | Raw data | 0 | 1.5 | ± 3.1 | |
| | Standardized | 0 | 2.0 | ± 3.7 | 0.86 |

5 Conclusions

In the present study, identifications of the location and size of a delamination crack of laminated graphite/epoxy plates are performed

using the electric resistance change method with response surface. The new data processing method using standardizations is adopted here, and the new method is applied to the experimental results. Cross-ply laminates and quasi-isotropic laminates

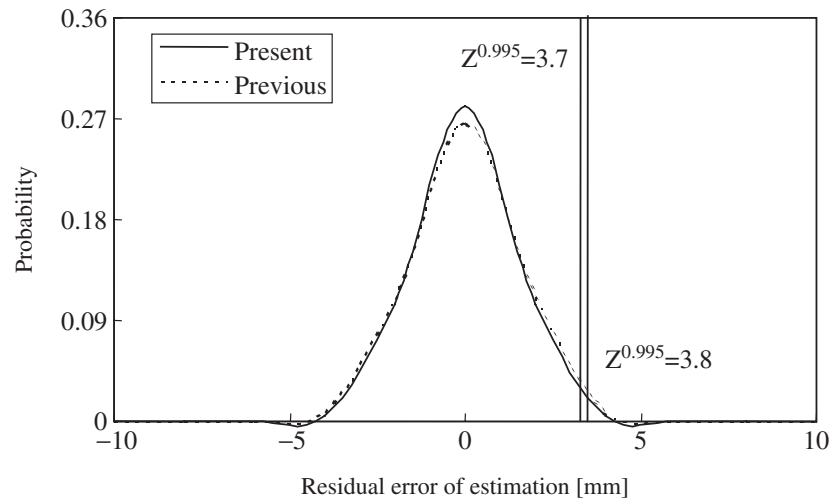


Figure 16 Error band of estimation of delamination size for cross-ply laminate.

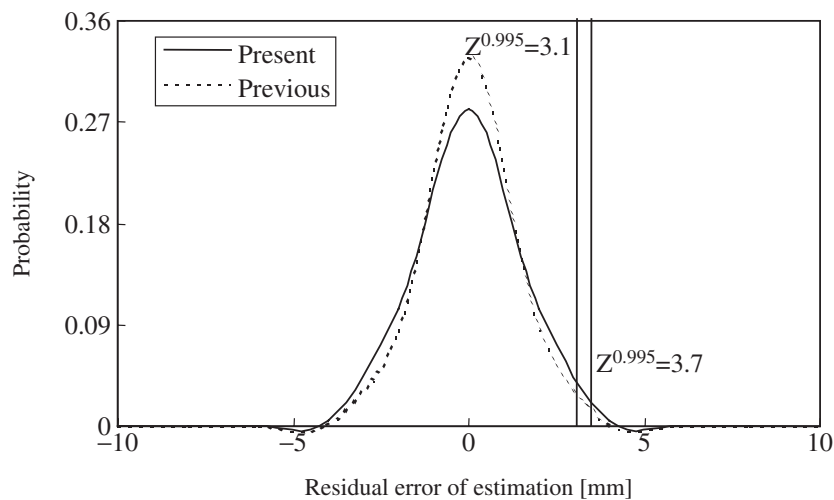


Figure 17 Error band of estimation of delamination size for quasi-isotropic laminate.

are prepared for experiments. The results obtained are as follows:

1. Even for the experimental data including experimental errors, the new method using standardizations shows excellently high performance of estimations of delamination size and locations.
2. Identification of delamination size and location with response surfaces can be successfully performed for both types of laminates.
3. By using modified electric resistance method, error band for estimations are also 2.5 times improved on identification of delamination location.

References

1. Moriya, K. and Endo, T. (1988). A study on flaw detection method for CFRP composite laminates (1st Report) The measurement of crack extension in

- CFRP composites by electrical potential method. *Aeronautical and Space Science Japan* 36(410), 139–146 (in Japanese).
2. Schulte, K. and Baron, C.H. (1989). Load and failure analyses of CFRP laminates by means of electrical resistively measurements. *Composite Science and Technology*, 36, 63–76.
 3. Muto, N., Yanagida, H., Miyayama, M., Nakatsuji, T., Sugita, M. and Ohtsuka, Y. (1992). Foreseeing of fracture in CFGFRP composites by measuring electric resistance. *J. of the Japan Society for Composite Materials*, 18(4), 144–150 (in Japanese).
 4. Fischer, Chr. and Arendts, F.J. (1993). Electrical crack length measurement and the temperature dependence of the mode I fracture toughness of carbon fibre reinforced plastics. *Composite Science and Technology*, 46, 319–323.
 5. Chen, P.W. and Chung, D.D.L. (1993). Carbon fiber reinforced concrete for smart structures capable of non-destructive flaw detection. *Smart Mater. Struct.*, 2, 22–30.
 6. Kaddour, A.S., Al-Salehi, F.A. and Al-Hassani, S.T.S. (1994). Electrical resistance measurement technique for detecting failure in CFRP materials at high strain rate. *Composite Science and Technology*, 51, 377–385.
 7. Wolfiger, C. and Drechsler, K. (1994). Damage detection in composite materials by monitoring electrical impedance. In: *Proc. of the Int. Symp. on Advanced Materials for Lightweight Structures*, ESTEC, Noordwijk (ESA-WPP-070), pp. 677–782.
 8. Chen, P.W. and Chung, D.D.L. (1995). Carbon-fiber-reinforced concrete as intrinsically smart concrete for damage assessment during dynamic loading. *J. Am. Ceram. Soc.*, 78(3), 816–818.
 9. Wang, X. and Chung, D.D.L. (1997). Sensing delamination in a carbon fiber polymer-matrix composite during fatigue by electrical resistance measurement. *Polymer Composites*, 18(6), 692–700.
 10. Irving, P.E. and Thiagarajan, C. (1998). Fatigue damage characterization in carbon fibre composite materials using an electric potential technique. *Smart Materials and Structures*, 7, 456–466.
 11. Abry, J.C., Bochart, S., Chateaumoins, A., Salvia, M. and Giraud, G. (1999). In situ detection of damage in CFRP laminates by electric resistance measurements. *Composite Science and Technology*, 59, 925–935.
 12. Seo, D.C. and Lee, J.J. (1999). Damage detection of CFRP laminates using electrical resistance measurement and neural network. *Composite Structures*, 47, 525–530.
 13. Abry, J.C., Choi, Y.K., Chateaumoins, A., Dalloz, B. and Giraud, G. (2001). In-situ monitoring of damage in CFRP laminates by means of AC and DC measurements. *Composite Science and Technology*, 61, 855–864.
 14. Weber, I. and Schwartz, P. (2001). Monitoring bending fatigue in carbon-fiber/Epoxy composite strands: A comparison between mechanical and resistance techniques. *Composite Science and Technology*, 61, 849–853.
 15. Muto, N., Arai, Y., Shin, S.G., Matsubara, H., Yanagida, H., Sugita, M. and Nakatsuji, T. (2001). Hybrid composites with self-diagnosing function for preventing fatal fracture. *Composite Science and Technology*, 61, 875–883.
 16. Kupke, M., Schulte, K. and Schuler, R. (2001). Non-destructive testing of FRP by DC and AC electrical method. *Composite Science and Technology*, 61, 837–847.
 17. Schueler, R., Joshi, S.P. and Schulte, K. (2001). Damage detection in CFRP by electrical conductance mapping. *Composite Science and Technology*, 61, 921–930.
 18. Kubo, S., Kuchinishi, M., Sakagami, T. and Ioka, S. (2001). Identification of delamination in layered composite materials by the electric potential CT method, applied electromagnetics and mechanics. In: Takagi, T. and Uesaka, M. (eds), *Proc. of the 10th Int. Symp. on Applied Electromagnetics and Mechanics*, Japan Soc. Applied Electromagnetics and Mechanics, pp. 641–642.
 19. Todoroki, A., Matsuura, K. and Kobayashi, H. (1995). Application of electric potential method to smart composite structures for detecting delamination. *JSME International J., Series A*, 38(4), 524–530.
 20. Todoroki, A., Kobayashi, H. and Matsuura, K. (1997). Application of electrical potential method as delamination sensor for smart structures of graphite/epoxy. In: Inoue, K., Shen, S.I.Y. and Taya, M. (eds), *US-Japan Workshop on Smart Materials and Structures*, University of Washington TMS, pp. 47–54.
 21. Todoroki, A. (1997). Delamination detection by electric resistance change for graphite/PEEK composites. In: *Proceedings of the 5th Japan International SAMPE Symposium*, pp. 899–904.
 22. Todoroki, A., Suzuki, H., Kobayashi, H., Nakamura, H. and Shimamura, Y. (1998). Evaluation of orthotropic electrical resistance for delamination detection of CFRP by electrical potential method. *Transactions of the Japan Society of Mechanical Engineers Series A*, 64(622), 1654–1659 (in Japanese).
 23. Todoroki, A. and Suzuki, H. (2000). Health monitoring of internal delamination cracks for graphite/epoxy composites by electric potential method. *Applied Mechanics and Engineering*, 5(1), 283–294.
 24. Todoroki, A., Tanaka, Y. and Shimamura, Y. (1999). Response surface for delamination monitoring of graphite/epoxy composite using electric resistance

- change. In: Chang, F.K. (ed.), *Structural Health Monitoring 2000*, Technomic Publishing Co. Inc., Lancaster Basel, pp. 308–316.
25. Todoroki, A., Tanaka, Y. and Shimamura, Y. (2001). Electric resistance change method for identification of embedded delamination of CFRP plates. *Materials Science Research International*. Special Technical Publication-2, *JSMS*, 139–145.
 26. Todoroki, A., Tanaka, M. and Shimamura, Y. (2002). Measurement of orthotropic electric conductance of CFRP laminates and analysis of the effect on delamination monitoring with electric resistance change method. *Composite Science and Technology*, 62(5), 619–628.
 27. Todoroki, A. (2001). Effect of number of electrodes and diagnostic tool for delamination monitoring of graphite/epoxy laminates using electric resistance change. *Composite Science and Technology*, 61(13), 1871–1880.
 28. Todoroki, A., Tanaka, M. and Shimamura, Y. (2003). High performance estimations of delamination of graphite/Epoxy laminates with electric resistance change method. *Composites Science and Technology*, 63(13), 1911–1920.
 29. Todoroki, A., Tanaka, M. and Shimamura, Y. Electrical resistance change method for monitoring delaminations of CFRP laminates: effect of spacing between electrodes. *Composites Science and Technology*, 65(1), 37–46.
 30. Myers, R. and Montgomery, D.C. (1995). *Response Surface Methodology Process and Product Optimization Using Designed Experiments*. New York: Wiley Interscience Publication.
 31. Suemasu, H. and Majima, O. (1998). Multiple delaminations and their severity in nonlinear circular plate subjected to transverse loadings, *J. Composite Materials*, 32(2), 123–140.